Principal interactions in the magnetic system $Fe_{1-x}Co_xSi$: Magnetic structure and critical temperature by neutron diffraction and SQUID measurements

S. V. Grigoriev,[1] S. V. Maleyev,[1] V. A. Dyadkin,[1] D. Menzel,[2] J. Schoenes,[2] and H. Eckerlebe[3]
[1]*Petersburg Nuclear Physics Institute, Gatchina, 188300 St. Petersburg, Russia*
[2]*Institut für Physik der Kondensierten Materie, TU Braunschweig, 38106 Braunschweig, Germany*
[3]*GKSS Forschungszentrum, 21502 Geesthacht, Germany*
(Received 11 July 2007; revised manuscript received 7 August 2007; published 27 September 2007)

The compound $Fe_{1-x}Co_xSi$ is a good representative for a cubic magnet with Dzyaloshinskii-Moriya interaction. On the basis of the neutron diffraction and superconducting quantum interference device measurements, we built the *H-T* phase diagram for the compound with different x from 0.1 to 0.7. The same set of parameters governs the magnetic system for different x. These parameters are well interpreted in the framework of the recently developed theory [S. V. Maleyev, Phys. Rev. B **73**, 174402 (2006)]. As a result, the spin-wave stiffness, the Dzyaloshinskii constant, the anisotropic exchange constant, and the spin-wave gap caused by the Dzyaloshinskii interaction have been obtained and plotted as a function of x. The changes of the magnetic structure with x can be well interpreted on the basis of our findings.

DOI: 10.1103/PhysRevB.76.092407 PACS number(s): 75.40.−s, 61.12.Ex

One of the most interesting problems in condensed matter physics in the past decade is the paradigm of quantum phase transitions (QPTs). In particular, MnSi, the cubic magnet with Dzyaloshinskii-Moriya (DM) interaction, has attracted much of the researchers' attention. This MnSi system is known to suffer the QPT under hydrostatic pressure P as the magnetic order disappears upon the increase of P ($T_C \to 0$ at $P \to P_c \approx 15$ kbar).[1,2] In spite of the great interest, neither the role played by the DM instability in this QPT was clarified nor any other parameter, which is responsible for the QPT, has been established. Similar to the pressure effect in MnSi, the variation of the cobalt concentration x in the compound $Fe_{1-x}Co_xSi$ results in a strong change of T_C. Therefore, the study of the principal interactions, their interplay, and their relation to T_C in $Fe_{1-x}Co_xSi$ would shed a new light on the QPT in MnSi and relative systems. On the other hand, the recent study of a single atomic layer of manganese on tungsten demonstrated the existence of the spin spiral structure with the long period of 12 nm instead of antiferromagnetic ordering, which is characteristic for Mn. This observation was interpreted through the appearance of the DM interaction on magnetic surfaces because such surface lacks obviously the inversion symmetry.[3] This finding changes the whole concept of the magnetic structures in nanomagnetism as it introduces a new important DM interaction into the consideration of the nano-object's properties. The theoretical approach, which is applied to explain this phenomenon, is similar to that made by Bak and Jensen[4] for the interpretation of the spiral structure in MnSi. Therefore, new theoretical and experimental efforts to describe and to understand the fascinating behavior of MnSi-type compounds are of great interest as they become the model systems for magnetic low-dimensional and nanoscale objects.

It is well known that the cubic B20-type compound $Fe_{1-x}Co_xSi$ orders in a one-handed spin helical structure.[5–8] In analogy to the magnetic structure of MnSi (Refs. 9 and 10) and FeGe,[11] the helicity is induced by an antisymmetric Dzyaloshinskii-Moriya exchange interaction caused by the lack of a center of symmetry in the arrangement of the magnetic atoms Fe and Co.[4,12,13] This DM interaction is isotropic in cubic crystals, and a weak anisotropic exchange (AE) interaction along with cubic anisotropy should fix the direction of the magnetic spiral.[4] In $Fe_{1-x}Co_xSi$, the helix wave vector **k** shows a weak tendency to orient along the [100] axis. Upon the increase of the Co concentration, this tendency disappears as a result of disorder, arising due to Co-to-Fe substitution, which destroys the local cubic symmetry. FeSi is a narrow-gap semiconductor with a band gap of about 30 meV (Ref. 14) and a nonmagnetic ground state.[15] The $Fe_{1-x}Co_xSi$ compounds remain paramagnetic for $0 < x < 0.05$, while at $x \in [0.05, 0.8]$, they order magnetically and become metallic.[14,16] The pure CoSi is, however, a diamagnetic semimetal.[17] Thus, the magnetic and transport properties of these compounds are strongly correlated, showing also a positive magnetoresistive effect in the ordered phase.[18] The critical temperature T_C for different concentrations x is plotted in Fig. 1. This Brief Report is aimed at estimating the principal interactions that determine the magnetic structure and discussing their relation to the value of the critical temperature T_C.

The magnetic properties of the $Fe_{1-x}Co_xSi$ single crystals (x=0.10, 0.15, 0.20, and 0.50 at. %) under an applied magnetic field were studied in detail. The samples were magnetically characterized by superconducting quantum interference device magnetometry, and their magnetic structure was studied by small angle neutron diffraction. From the diffraction experiment, one can build the magnetic phase diagram shown in Figs. 2(a)–2(c) for $Fe_{0.85}Co_{0.15}Si$, $Fe_{0.8}Co_{0.2}Si$, and

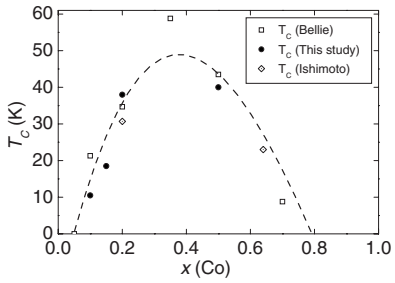

FIG. 1. Critical temperature T_C as function of the Co concentration x (□, Refs. 5 and 6; △, Refs. 7 and 8; and ●, this study).

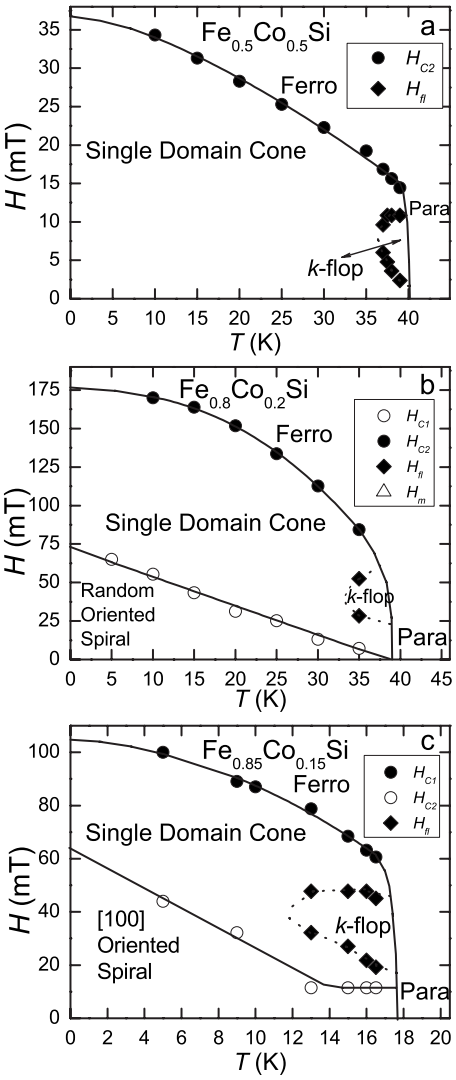

FIG. 2. H-T phase diagram for (a) $Fe_{0.5}Co_{0.5}Si$, (b) $Fe_{0.8}Co_{0.2}Si$, and (c) $Fe_{0.85}Co_{0.15}Si$. For all three Co concentrations, the compound is paramagnetic above T_C. Below T_C and at $H<H_{C1}$, a spiral spin structure occurs with the **k** vector either oriented randomly or along the ⟨100⟩ direction. Different domains tend to orient along the field axis in the region between H_{C1} and H_{C2}. Above H_{C2}, the sample orders ferromagnetically.

$Fe_{0.5}Co_{0.5}Si$, respectively. These phase diagrams are very similar and can be described by the same set of parameters H_{C1}, H_{C2}, and H_{fl}.

The magnetic structure of $Fe_{1-x}Co_xSi$ in the absence of an applied field consists of spiral domains with the wave vector **k**, which is either randomly oriented for some concentrations or has a slight preference to orient along the cube edges: $\mathbf{k}\|\langle 100\rangle$. The value of **k** changes with the concentration, but does not change with the temperature. The applied magnetic field tends to reorient the helix wave vectors of different domains along the field axis. The process of the reorientation starts from the threshold field H_{C1} when the interaction of the helix with the magnetic field becomes stronger than the local anisotropy of the system. In the scattering, this is reflected through a concentration of the scattering intensity along **H** when the single domain conical structure is formed. This single domain structure remains stable up to the critical field H_{C2} when the transition from the conical state into the ferromagnetic state occurs. In addition, a **k** flop of the helix wave vector was found in a certain field range and slightly below T_C, similar to that observed in MnSi.[19] The **k** flop is seen in the diffraction experiment as a 90° jump of the wave vector from $\mathbf{k}\|\mathbf{H}$ to $\mathbf{k}\perp\mathbf{H}$. Going deeper into the **k**-flop phase, the intensity of the Bragg reflection at $\mathbf{q}=k\|\mathbf{H}$ decreases, while a new Bragg spot appears at $\mathbf{k}\perp\mathbf{H}$. The field H_{fl} shows the boundary of the new **k**-flop phase. The field value associated with the absolute minimum of the intensity for $\mathbf{k}\|\mathbf{H}$ is denoted as H_{gap}, in accordance with interpretation given below. These phase diagrams (Fig. 2) are well interpreted within the theory recently developed by one of the authors[20] on the basis of the Bak-Jensen model.[4] We present the essence of this theory below.

We take into account the following interactions: conventional isotropic exchange (J), DM interaction (DM), the anisotropic exchange (AE) interaction, cubic anisotropy (C), and the Zeeman interaction with the magnetic field, assuming the hierarchy $J \gg DM \gg AE \sim C$. In accordance with Refs. 4 and 12, the helical order is stabilized due to conventional exchange and DM interactions, and the helix wave vector is defined as

$$k = SD/A, \tag{1}$$

where D is the strength of the DM interaction and A is the spin-wave stiffness at momenta $q \gg k$.

The orientation of the helix vector **k** relative to the crystal axes is governed by the anisotropic energy

$$E_{an} = \left(\frac{S^2Fk^2}{2} - \frac{3S^4K}{8}\right)L, \tag{2}$$

where F and K are constants determining the strength of the anisotropic exchange and cubic anisotropy, respectively. $L = 1 - \Sigma_{i=x,y,z} k_i^4/k^4$ is a cubic invariant with two extrema equal to 2/3 and zero for the vector **k** along the ⟨111⟩ and ⟨001⟩ directions, respectively.

In Ref. 20, the ground state energy in the magnetic field and the spin-wave (SW) spectrum were evaluated. It is shown that the helical systems with the DM interaction are unstable with respect to the small magnetic field applied perpendicular to **k** unless they are stabilized by a small gap in the spin-wave spectrum Δ. The magnetic field depending part of the ground state energy for small fields $g\mu_B H < \Delta\sqrt{2}$ is given by[20]

$$E_H \approx -\frac{Sg\mu_B}{2H_{C2}}\left\{H_\parallel^2 + \frac{H_\perp^2\Delta^2}{2[\Delta^2 - (1/2)(g\mu_B H_\perp)^2]}\right\}, \tag{3}$$

where $H_\parallel$ and $H_\perp$ are the field components parallel and perpendicular to the helix wave vector **k**. The first term with $H_\parallel$ is a classical part of the Zeeman energy. The second one has a quantum origin, and it describes the interaction of the field, perpendicular to **k**, with the helix as an individual entity. For small fields $g\mu_B H \leqslant \Delta\sqrt{2}$, the major contribution to the spin-wave gap is due to DM interaction, which breaks the total spin conservation law. The second term in Eq. (3) results in the appearance of the **k**-flop phase near T_C at $H \sim H_{gap}$ (Fig.

2) when the perpendicular configuration of **k** with respect to the field axis becomes energetically more favorable than the parallel one. The detailed analysis of this phenomenon is given in Ref. 19. The important consequence of Eq. (3) is that the spin-wave gap can be experimentally estimated near T_C,

$$\Delta \simeq g\mu_B H_{gap}/\sqrt{2}. \tag{4}$$

The perpendicular configuration of the helix in the field becomes unstable if $g\mu_B H_\perp \geqslant \sqrt{2}\Delta$, and hence, above this field, the helix wave vector has to be oriented along the field. For a complete analysis of the **k** rotation, one has to study the evolution of the minimum of $E_{an}+E_H$ as function of the **k** direction.[21]

According to the theory,[20] for small fields, the SW gap stems from the spin-wave interaction only. It is temperature independent and given by

$$\Delta_{SW} = c(SD)^2/2A, \tag{5}$$

where c has to be smaller than unity.

After **k** has rotated along the field direction, the helix transforms into a field-induced ferromagnet at the critical field[20]

$$g\mu_B H_{C2} = Ak^2, \tag{6}$$

where A is the spin-wave stiffness at $q \gg k$.

The theory given above was first applied to MnSi.[22] Particularly, it was shown that the value of the stiffness $A_m = 50$ meV Å^2 measured by three-axis spectroscopy for $T = 5$ K (Ref. 10) coincides practically with the value estimated from Eq. (6): $A_{est} = 50$ meV Å^2. Thus, the validity of this expression [Eq. (6)] was proven experimentally. Accounting for the fact that Eq. (1) is the definition, one is able, from the parameters of the magnetic structure measured in the experiment (k, H_{gap}, and H_{C2}), to calculate the major driving interactions of the magnetic system, such as the spin-wave stiffness $A = g\mu_B H_{C2}/k^2$, the Dzyaloshinskii constant $SD = Ak$, and the spin-wave gap $\Delta \sim g\mu_B H_{gap}/\sqrt{2}$.

It should be noted that $Fe_{1-x}Co_xSi$ has the same, as MnSi, crystallographic structure without a symmetry center and the same magnetic helical structure based on DM interaction. The similarity of the magnetic structures is pointed out by the magnetic H-T phase diagrams, which are very much similar for both systems. Therefore, we suppose that the theory applicable to MnSi should also be valid in the case of $Fe_{1-x}Co_xSi$.

We have revisited the $Fe_{1-x}Co_xSi$ system in order to obtain values of the principal interactions as a function of Co concentration x. The investigations performed for different Co concentrations show a similar behavior characterized by the fields H_{C2} and H_{gap}, and the helix wave vector **k**. We plot these parameters as function of the Co concentration x in Fig. 3. For completeness, we used also the values of these parameters as obtained by Beille *et al.* in Refs. 5 and 6, and by Ishimoto *et al.* in Refs. 7 and 8. As seen from Fig. 3(a), the length of **k** increases at small x, has a maximum at $x \sim 0.2$, and finally decreases smoothly, approaching zero at $x \approx 0.8-0.9$. The x dependence of H_{C2} [Fig. 3(b)] and H_{gap} [Fig. 3(c)] demonstrates a similar behavior.

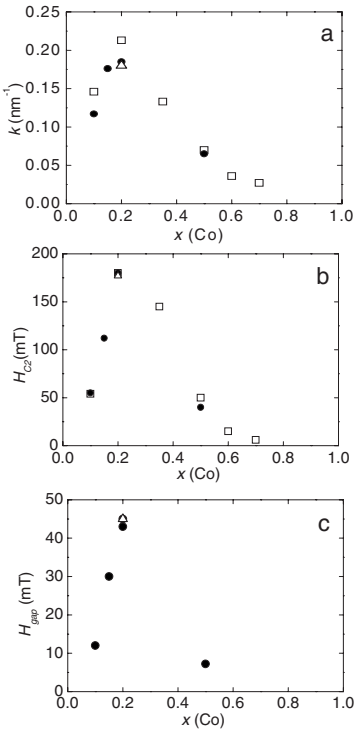

FIG. 3. Dependence of (a) the helix wave vector k, (b) the critical magnetic field H_{C2}, and (c) the **k**-flop field H_{gap} on the Co concentration x for $Fe_{1-x}Co_xSi$ (□, Refs. 5 and 6; △, Refs. 7 and 8; and ●, this study).

As shown above, one can obtain the principal interactions of the system from these experimental parameters using Eqs. (1), (4), and (6). Figure 4 shows the dependence of the energies A/a^2, SD/a, and Δ on the concentration x. The exchange energy A/a^2 rises smoothly with increasing x, showing no maximum [Fig. 4(a)]. All experimental values, except for $x=0.7$, follow a straight line, which gives the value $A = 0.9$ meV when extrapolating to $x=0$. Thus, one can conclude that the transition temperature T_C shown in Fig. 1 is not directly related to the exchange energy A/a^2. Opposite to this, the DM interaction Da increases with increasing Co concentration x, has a maximum at $x=0.35$, and decreases to zero at $x \approx 0.8$. Thus, the value of the DM interaction [Fig. 4(b)] follows the x dependence of T_C (Fig. 1) and is, likely, related to the T-x phase diagram of this compound.

The behavior of the spin-wave gap Δ as function of x is similar to that of the DM interaction [Fig. 4(c)]. In particular, an extrapolation of Δ to the small-x range gives a value of $\Delta \approx 0$ at $x \approx 0.05$, and it also decreases for large x. Testing the hypothesis on the origin of the SW gap, we plot the values of Δ calculated from Eq. (5) using the parameters A and SD obtained from the experiment [smooth curve in Fig. 4(c)]. It is seen that the calculated curve [Eq. (5)] represents the experimental values obtained from H_{gap} for $c=0.33$. This, indeed, evidences that the SW gap is caused by the spin-wave interaction mediated by the DM interaction. On the other hand, one can conclude from our data that the SW gap Δ is not directly related to the value of the critical temperature T_C because, for example, at $x=0.5$, the SW gap is very small, whereas $T_C = 38$ K is relatively high [see Figs. 4(c) and 1, respectively].

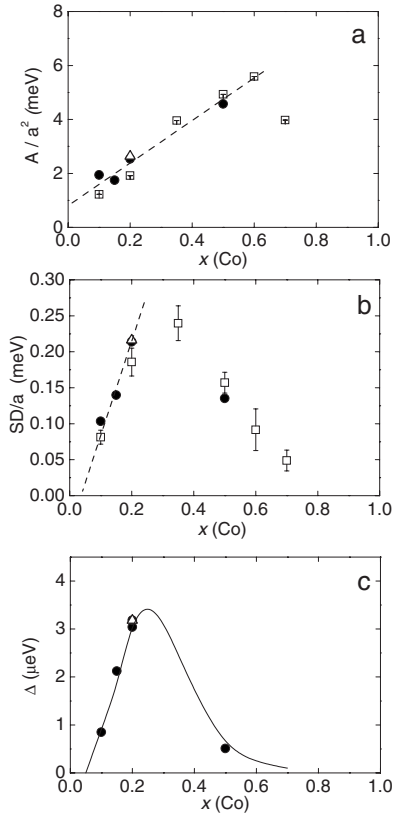

FIG. 4. Dependence of the (a) exchange energy of the order A/a^2, (b) DM energy SD/a, and (c) the spin-wave gap Δ on the Co concentration x for $Fe_{1-x}Co_xSi$. The points show the parameters calculated from the data taken from Refs. 5 and 6 (□), from Refs. 7 and 8 (△), and from this study (●).

In our view, the SW gap is responsible for the stability of the perpendicular (field-to-helix wave vector) configuration but not for the stability of the helix structure itself. Thus, the small SW gap value leads only to the orientation of **k** along the field axis at a rather small field as is observed at $x=0.5$.[21,23]

The obvious relation between T_C and the DM interaction *SDa* can be explained by the following consideration: It is known that the DM interaction is caused by the first order spin-orbit coupling. We suppose that the substitution of Fe by Co results in a special nearest-neighbor configuration (Fe-Fe-Co), producing this spin-orbit coupling of the electron clouds. Such spin-orbit coupling occurs neither for (Fe-Fe-Fe) nor for (Co-Co-Co) nearest-neighbor configurations. Naturally, this leads to the maximum DM interaction at $x=0.33$ and to the maximum ordering temperature of the helix structure caused by this interaction. The detailed picture is not clarified yet.

We have applied a recently developed theory for cubic magnets with the Dzyaloshinskii-Moriya interaction[20] in order to interpret the results of experiment on $Fe_{1-x}Co_xSi$. We evaluated the major interactions of the system (A, SDa, and the spin-wave gap Δ) from our diffraction experiments using the theory mentioned above.

(1) From the critical field H_{C2} and the helix wave vector k, we obtained the exchange energy as $A/a^2 \approx g\mu_B H_{C2}/k^2a^2$. The monotonous dependence of A/a^2 on the concentration x demonstrates the absence of any correlation between this parameter and the critical temperature T_C. The latter shows a slightly asymmetric bell-like shape as function of the Co concentration x, with a maximum at $x \sim 0.35$.

(2) The DM interaction $SD=Ak$ was also obtained. Its x dependence resembles the behavior of T_C showing that the DM interaction is, *likely*, responsible for the critical temperature of these compounds.

(3) The spin-wave gap $\Delta \sim g\mu_B H_{fl}/\sqrt{2}$ was derived. It is shown that (i) the SW gap is caused by the DM interaction and (ii) its value is proportional to $D^2/2A$, in accordance with the theoretical predictions.

S.V.G., S.V.M., and V.A.D. acknowledge GKSS for their hospitality. The work is supported in part by the RFBR (Projects Nos. 05-02-19889, 06-02-16702, and 07-02-01318) and the Russian State Programs "Quantum Macrophysics," "Strongly Correlated Electrons in Semiconductors, Metals, Superconductors, and Magnetic Materials," and "Neutron Research of Solids."

[1] C. Pfleiderer, S. R. Julian, and G. G. Lonzarich, Nature (London) **414**, 427 (2001).
[2] C. Pfleiderer *et al.*, Nature (London) **427**, 227 (2004).
[3] M. Bode *et al.*, Nature (London) **447**, 05802 (2007).
[4] P. Bak and M. H. Jensen, J. Phys. C **13**, L881 (1980).
[5] J. Beille, J. Voiron, and M. Roth, Solid State Commun. **47**, 399 (1983).
[6] J. Beille *et al.*, J. Phys. F: Met. Phys. **11**, 2153 (1981).
[7] K. Ishimoto *et al.*, J. Magn. Magn. Mater. **90&91**, 163 (1990).
[8] K. Ishimoto *et al.*, Physica B **213&214**, 381 (1995).
[9] Y. Ishikawa, K. Tajima, D. Bloch, and M. Roth, Solid State Commun. **19**, 525 (1976).
[10] Y. Ishikawa, G. Shirane, J. A. Tarvin, and M. Kohgi, Phys. Rev. B **16**, 4956 (1977).
[11] B. Lebech, J. Bernhard, and T. Freltoft, J. Phys.: Condens. Matter **1**, 6105 (1989).
[12] I. E. Dzyaloshinskii, Zh. Eksp. Teor. Fiz. **46**, 1420 (1964).
[13] D. Nakamishi, A. Janase, A. Hasejawa, and M. Kitaoka, Solid State Commun. **35**, 995 (1980).
[14] D. Zur *et al.*, Phys. Rev. B **75**, 165103 (2007).
[15] V. Jaccarino *et al.*, Phys. Rev. **160**, 467 (1976).
[16] D. Menzel, D. Zur, and J. Schoenes, J. Magn. Magn. Mater. **272-276**, 130 (2004).
[17] J. H. Wernick, G. K. Wertheim, and R. C. Sherwood, Mater. Res. Bull. **7**, 1431 (1972).
[18] N. Manyala *et al.*, Nature (London) **404**, 581 (2000).
[19] S. V. Grigoriev *et al.*, Phys. Rev. B **73**, 224440 (2006).
[20] S. V. Maleyev, Phys. Rev. B **73**, 174402 (2006).
[21] S. V. Grigoriev *et al.*, J. Phys.: Condens. Matter **19**, 145286 (2007).
[22] S. V. Grigoriev *et al.*, Phys. Rev. B **74**, 214414 (2006).
[23] M. Uchida, Y. Onose, Y. Matsui, and Y. Tokura, Science **311**, 359 (2006).